

Door-guided indoor space segmentation via progressive geometric analysis

Seung H. Song^{1c}, Seokju Shin^{1d}, Changsu Lee^{2b}, Heejae Ahn^{2b}, Seungjun Kim^{1a} and Hunhee Cho^{*1}

¹Department of Civil, Environmental and Architectural Engineering, Korea University, Seongbuk-Gu, Seoul 02841, Republic of Korea

²Department of Civil and Environmental Engineering, University of Alberta, 9211-116 Street, Edmonton, Alberta T6G 2H5, Canada

(Received June 2, 2025, Revised July 10, 2025, Accepted July 11, 2025)

Abstract. Point cloud segmentation is crucial for Forensic Information Modeling (FIM) and Building Information Modeling (BIM) applications; however, existing methods either require extensive training data (deep learning) or struggle in complex architectural layouts (geometry-based). This paper presents a door-guided geometric framework that achieves robust indoor space segmentation without learned features. The approach introduces four preprocessing modules: 1) door gap detection through cross-sectional analysis (requiring only 4 manual clicks to identify all doors in a building), 2) corridor isolation via principal component analysis, 3) tile-based structural filtering, and 4) verticality-based wall extraction. These modules establish spatial boundaries before applying hierarchical watershed segmentation with multi-scale spillage prevention. Validated on the S3DIS Area 6 dataset (27 rooms, 1.17 million points), the framework achieved an average IoU of 96.5% and an F1-score of 98.0%, matching deep learning performance while eliminating training requirements. The purely geometric approach enables deployment in forensic engineering contexts where training data is unavailable and computational resources are limited, directly supporting damage assessment and structural investigation workflows.

Keywords: door-guided framework; geometric segmentation; indoor segmentation; watershed algorithm

1. Introduction

Forensic Information Modeling (FIM) facilitates detailed assessments of defects and failures in infrastructure by integrating Building Information Modeling (BIM) principles (Brando *et al.* 2013). Accurate as-damaged representations are effectively stored in a visualized 3D database, thereby streamlining forensic investigation processes. Accordingly, the quality of BIM generation directly affects the reliability of damage assessments. A critical factor for high-quality BIM is the accuracy of spatially relevant and context-rich segmentation within point clouds—sets of data points in spatial coordinates, typically generated using laser scanning or photogrammetry. In their raw state, point clouds consist of unstructured clusters of millions of 3D coordinates, lacking the spatial context necessary for targeted, room-level assessments (Wang and Kim 2019, Poux *et al.* 2022).

The quality of BIM generation directly affects the reliability of damage assessments. This enables the association of defects with well-defined spatial regions in BIM, facilitating contextualized damage analysis and communication in forensic engineering tasks. Specifically, accurate room-level segmentation provides the spatial framework necessary for: 1) localizing detected defects to

specific rooms or zones, enabling targeted structural assessments, 2) quantifying damage extent by calculating affected areas within each segmented space, and 3) generating room-by-room inspection reports that link structural anomalies to their precise spatial contexts. Without reliable indoor space segmentation, defect data remains spatially ambiguous, hindering systematic forensic analysis and remediation planning.

Broadly, recent advancements in point cloud segmentation are threefold: 1) deep-learning-based semantic methods, 2) geometry-based methods, and 3) hybrid methods that combine both semantic and geometric techniques. Among these, deep learning approaches have garnered significant attention due to their potential for automated feature extraction. However, they typically require extensive training data and high computational resources, making them less practical for deployment in forensic settings (Hu *et al.* 2024, Patil and Kalantari 2025). Geometry-based methods, on the other hand, tend to generalize well across diverse structural forms but often struggle with complex architectural layouts (Sahin 2015, Thomson and Boehm, 2015).

Tang *et al.* (2024) proposed a geometry-centric alternative that integrates 2D and 3D constraints based on point cloud density and elevation distribution. Their framework achieved near-perfect segmentation accuracy in standard rooms by combining vertical structure extraction, adaptive space anchor identification, and hierarchical contour-based partitioning. Nevertheless, the method's performance suffered from degradation in scenes with narrow corridors due to fixed morphological parameters. Hybrid approaches have since emerged to mitigate such issues by incorporating learned semantic anchors alongside

*Corresponding author, Professor

E-mail: hhcho@korea.ac.kr

^aProfessor

^bPh.D.

^cPh.D. Student

^dM.Sc. Student

geometric refinements. For example, Tang *et al.* (2022) and Fang *et al.* (2021) utilized deep learning to classify walls and doors prior to applying morphological segmentation. While these hybrid methods improve segmentation continuity, they inherit the limitations of deep learning, particularly in terms of data dependence and noise sensitivity (Ma *et al.* 2020, Li *et al.* 2024). More recently, Song *et al.* (2024) proposed using learned door seeds as structural anchors for region growing, further enhancing alignment with architectural features. Nevertheless, this approach still relies on pre-trained models, potentially limiting scalability in sparse or heterogeneous forensic datasets.

Despite these advances, three critical gaps constrain current approaches in forensic engineering contexts. First, training data scarcity poses a fundamental challenge. Point clouds from damaged or aging infrastructure are inherently sparse and unstructured, with occlusions from debris, missing sections from structural damage, and irregular geometries that deviate from training distributions. Manual annotation of such data is not only labor-intensive but also error-prone, as even experts struggle to delineate room boundaries in partially collapsed structures. This makes supervised learning approaches impractical for forensic applications where each building presents unique deterioration patterns. Second, architectural layout complexity extends beyond standard rectilinear designs. Real-world forensic scenarios encounter narrow corridors that connect multiple spaces, curved walls in historical buildings, irregular room geometries from renovations, and nested configurations where rooms exist within larger spaces. Current methods, particularly those assuming Manhattan World geometries, fail to segment such layouts accurately, leading to merged rooms or fragmented spaces.

Third, computational resource limitations restrict field deployment. Forensic engineers often work in environments where real-time processing is essential but high-performance hardware is unavailable. GPU-dependent deep learning models require computational resources that exceed typical field laptops, while cloud processing introduces latency and connectivity dependencies unsuitable for on-site assessments.

To address these limitations while maintaining the interpretability and efficiency required for forensic applications, this study presents a novel geometry-based approach. Building on recent geometry-based strategies—such as the framework by Tang *et al.* (2024), which underscored the potential of multi-dimensional geometric cues—this study introduces four critical innovations to geometry-based segmentation: 1) A preprocessing pipeline with explicit door gap detection that provides reliable spatial anchors without learned features, 2) Tile-based structural filtering that separates structural elements (walls, floors, ceilings) from non-structural elements, enabling cleaner segmentation boundaries, 3) Corridor-specific segmentation that addresses the narrow space challenge identified by Tang *et al.* (2024), and 4) An advanced watershed partitioning incorporating multi-scale spillage prevention mechanisms designed to minimize over-segmentation in complex layouts.

The remainder of this paper is structured as follows: Chapter 2 reviews related literature in point cloud segmentation. Chapter 3 presents the proposed methodology, including the preprocessing pipeline and enhanced watershed segmentation. Chapter 4 validates the approach through experiments on standard benchmarks and forensic case studies. Chapter 5 discusses key findings, limitations, future directions, and conclusions. This study addresses all three gaps through a purely geometric approach that: 1) eliminates training data requirements through door-guided geometric constraints, 2) handles complex layouts via explicit corridor isolation and hierarchical contour analysis, and 3) achieves computational efficiency suitable for CPU-only field deployment.

2. Literature review

Point cloud data (PCD) plays a critical role in digitally representing the three-dimensional geometry and constituent components of indoor environments. Due to its nature as unstructured data consisting solely of point coordinates, a preprocessing step is essential to organize it into structured units before analysis and modeling. Segmentation is the process of partitioning the point cloud according to spatial or spectral attributes to group points into semantically meaningful structural units, providing a foundation for BIM reconstruction (Song *et al.* 2024, Poux *et al.* 2022, Wang and Kim 2019). Segmentation techniques for point clouds are broadly categorized into geometry-based, deep learning-based, and hybrid approaches.

Geometry-based segmentation utilizes geometric properties, such as spatial position, orientation, and point density, to isolate primary architectural components. These methods can be further divided into plane-based approaches and morphology-based techniques. Plane-based approaches have been extensively adopted due to their effectiveness in processing artificial environments. Sahin (2015) proposed a mathematical filtering approach to distinguish planar surfaces at varying depths by computing point-to-plane distances. Thomson and Boehm (2015) used RANSAC to detect dominant planes, followed by Euclidean clustering to segment intra-planar objects. Ochmann *et al.* (2016, 2019) developed methods for room segmentation by treating it as a labeling problem, though these approaches struggled with obstructed spaces. Similarly, Wang *et al.* (2015) segmented 3D point clouds into planes and utilized boundary detection to classify structures; however, this approach remained susceptible to interference from furniture. Morphology-based methods assume that spaces are segmented by vertical structures, employing techniques such as distance transform (Fabbri *et al.* 2008), contour detection (Gong *et al.* 2018), and watershed segmentation (Singh & Frevert, 2003). Jung *et al.* (2017) proposed a morphology-based space partition, which creates initial segment maps and iteratively connects skeletonized walls. Hübner *et al.* (2021) applied similar techniques using triangular meshes. However, these methods often neglect curved structures, resulting in under-segmentation. There also have been

studies that examined more sophisticated geometric segmentation approaches. For instance, Li *et al.* (2018) performed a z-axis distribution analysis to distinguish floor levels, applying morphological operations for spatial labeling. Kim *et al.* (2023) extracted edge features and constructed 2D floorplans using concave hull techniques. Bae and Kim (2023) applied 2D projection with DBSCAN clustering to isolate structural elements. The Manhattan World assumption presupposes that architectural surfaces align with three orthogonal axes, with walls expected to be perfectly vertical and perpendicular to each other (Coughlan and Yuille, 1999). While this assumption simplifies plane detection and segmentation in idealized environments, it fails in real-world buildings featuring curved walls, non-perpendicular intersections, slanted surfaces, and irregular renovations, which are conditions prevalent in forensic engineering assessments.

While geometry-based methods offer automation and structural clarity, they face significant limitations: 1) dependence on Manhattan World assumptions, 2) poor handling of curved or non-planar structures, 3) sensitivity to noise and occlusions, and 4) difficulty with complex nested or circular configurations (Nikooohemat *et al.* 2020, Tran and Khoshelham 2020).

Deep learning techniques have garnered significant attention due to their ability to automate feature extraction (Hu *et al.* 2024). Depending on the needs, these approaches can be adopted for single-room recovery or large-scale segmentation techniques. For single-room recovery, image-based reconstruction was initially adopted. The DeLay framework (Dasgupta *et al.* 2016) employed FCNNs to detect ceilings, walls, and floors from images. RoomNet (Lee *et al.* 2017) introduced an end-to-end approach for room layout recovery through semantic segmentation. However, these methods struggle with multi-room or floor-wide segmentation. For multi-room, floor-wide, or large-scale segmentation, Liu *et al.* (2017, 2018) integrated 2D CNNs with 3D classification networks for structured reconstruction through corner extraction and integer programming. Chen *et al.* (2019) projected 3D point clouds into density maps using instance segmentation (He *et al.* 2017) for initial room partitioning. While achieving high accuracy on specific datasets (e.g., Beike), these methods exhibit poor generalization to diverse indoor spaces and struggle with circular or nested configurations. Point cloud-specific architectures have been developed to process 3D data directly. Park *et al.* (2022) utilized PointNet for point-wise feature extraction combined with DBSCAN clustering. Patil and Kalantari (2025) compared state-of-the-art models, including PointNeXt and Swin3D. Perez-Perez *et al.* (2021) introduced Scan2BIM-Net, an architecture that integrates CNN-RNN models for joint semantic and geometric processing.

Despite advances, deep learning methods face critical limitations: (1) heavy dependence on large annotated datasets, (2) poor generalization across different architectural styles, (3) computational intensity requiring GPU resources, (4) tendency to overlook small spaces, and (5) difficulty differentiating similar structural elements (Ma *et al.* 2020, Li *et al.* 2024).

To overcome the limitations and challenges of both geometry- and deep-learning-based segmentation, hybrid segmentation methods have been introduced to combine these methods strategically. Tang *et al.* (2022) and Fang *et al.* (2021) employed semantic segmentation for vertical structure detection, followed by morphological processing for space partition. Yang *et al.* (2021) utilized similar techniques combining semantic segmentation (Ronneberger *et al.*, 2015) with morphological algorithms.

Recent hybrid methods have explored various integration strategies. Mahmoud *et al.* (2025) performed initial semantic segmentation using deep learning, followed by geometric analysis for precise structural extraction. Song *et al.* (2024) proposed a more efficient approach that utilizes pre-trained PointNeXt as seeds for geometric segmentation, thereby improving alignment with architectural features.

While hybrid methods improve segmentation continuity and accuracy, they inherit limitations from both approaches: 1) continued reliance on training data for the deep learning component, 2) computational overhead from running multiple algorithms, 3) error propagation from incorrect semantic predictions, and 4) complexity in parameter tuning across different methods.

From conducting an extensive literature review, it was evident that there is a clear and rapid progression in point cloud segmentation approaches, ranging from pure geometric approaches to deep learning and hybrid techniques. Geometry-based segmentations are mostly interpretable; however, they tend to struggle with narrow corridors, circular structures, and nested configurations. Deep-learning-based segmentations enable automated feature learning; however, they suffer from low scalability. Accordingly, the hybrid-segmentation methods attempt to combine the strengths of both approaches but still face limitations in terms of computational overhead and training data requirements.

To address the limitations of the existing point cloud segmentation methods, this study introduces a purely geometric segmentation framework that builds on the innovations of Tang *et al.* (2024) and Song *et al.* (2024). The proposed framework adopts the door-seed concept but implements purely geometric door gap detection through cross-sectional analysis and density-based filtering. Additionally, rather than fixed morphological parameters that limit the applicability of earlier geometric methods, the framework adapts erosion radii, density thresholds, and overlap parameters based on local point cloud characteristics.

3. Methodology

3.1 Research approach

The framework specifically targets room-level space segmentation, partitioning indoor environments into functionally distinct rooms while excluding fine-grained component segmentation. Walls, floors, and ceilings are identified solely as boundary elements that define room

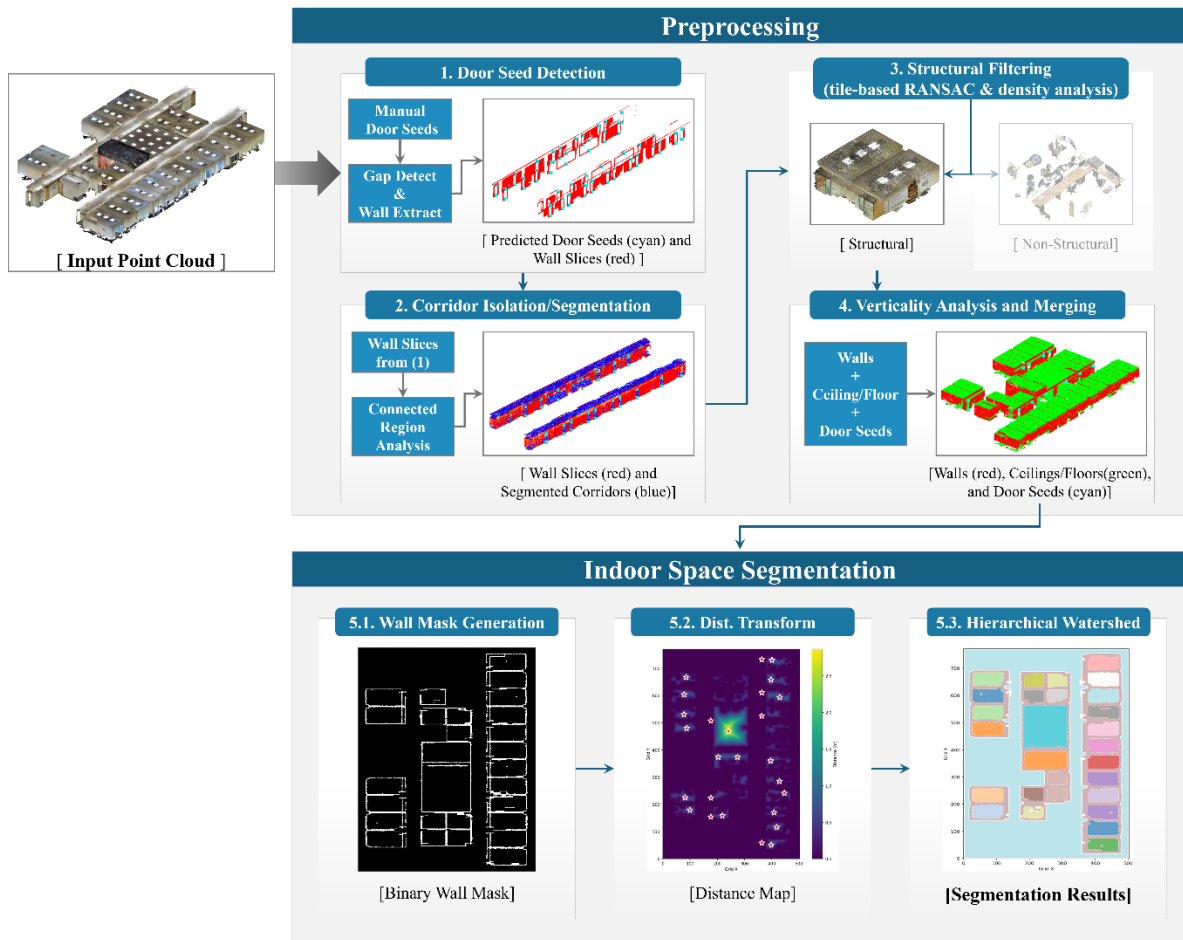


Fig. 1 Door-guided indoor space segmentation framework

extents, not as individual components for detailed modeling. This scope aligns with forensic damage assessment requirements, where room-level localization suffices for most structural evaluations. Column detection, furniture segmentation, and detailed architectural element modeling fall outside the scope, as they require component-specific processing beyond room boundary determination.

The framework aims to address the limitations of existing segmentation methods through a preprocessing-first approach that establishes robust spatial boundaries before actual indoor space segmentation. First, the framework processes the raw point clouds through four preprocessing modules followed by three main segmentation stages. The preprocessing phase extracts contextually relevant spatial elements and structural boundaries. The segmentation phase partitions the space using these spatial elements to achieve accurate room-level segmentation. The proposed framework is validated against the large-scale indoor PCD comprising 27 individual PCDs from Area 6 of the S3DIS dataset, which is an open-source dataset consisting of large-scale indoor PCDs frequently utilized for benchmarking PCD segmentation frameworks. The complete framework is depicted in Fig. 1

The four-module preprocessing pipeline directly addresses the identified research gaps: 1) eliminates training data dependency through purely geometric door gap detection via cross-sectional analysis, requiring only 4

manually marked points that automatically predict all door locations along the main building axes, rather than labeled training datasets, 2) handles architectural complexity through three mechanisms: a) corridor-specific isolation that prevents narrow spaces from causing room bleeding, b) tile-based structural filtering that adapts to local geometric variations without Manhattan World assumptions, and c) hierarchical watershed segmentation that recognizes nested spatial relationships, and 3) ensures computational efficiency as all modules utilize CPU-optimized operations including distance transforms, morphological operations, and local tile-based processing, enabling the framework to process 1.17 million points in under 30 seconds on a standard laptop CPU.

3.2 Preprocessing: Door seed detection

The preprocessing pipeline establishes fundamental spatial relationships that will be utilized in the subsequent guided segmentation. The preprocessing consists of four interconnected steps that refine the understanding of the indoor environment. In the first preprocessing step, door openings are predicted from manually marked seed points (four points total for the entire building - one click at each end of the main corridor axes, which automatically determines door locations for all rooms aligned along these axes). Door openings, as examined by Song *et al.* (2024),

can serve as meaningful spatial anchors that define transitions between indoor spaces. While Song *et al.* (2024)'s approach relies on pre-trained neural network that can be difficult to scale across different indoor settings, utilization of marked door openings enable purely geometric door gap detection through cross-sectional analysis. With the marked door openings, the door gap detection algorithm analyzes vertical cross-sections to identify gaps that satisfy door-like characteristics. For each wall at position x_w , the algorithm extracts points within a slice of width 2δ (where δ is a fixed value of 0.25 m) (Eq. (1)).

$$S_w = \{p \in P : |p_x - x_w| \leq \delta\} \quad (1)$$

Within this slice, a 2D occupancy grid gets constructed in the Y-Z plane with resolution r at 0.10 m. Then, the algorithm identifies empty regions by conducting connected component analysis following a binary morphological opening to remove noise as defined in Eq. (2.), where γ represents the opening operation within a 3×1 structural element.

$$M_{clean} = \gamma(M_{empty}) \quad (2)$$

Each detected gap region R_i , then gets validated for door opening candidacy based on three criteria: 1) height constraint of $1.6m \leq h \leq 2.5m$; 2) width constraint of

$0.7m \leq h \leq 1.2m$; and 3) floor proximity of $z_{bottom} \leq z_{floor} + 0.2m$.

Moreover, the algorithm performs recursive subdivision for wide openings to robustly handle various geometric conditions such as double doors and/or adjacent openings. Accordingly, each detected door opening corresponds to a single door. As a result, the output consists of pair of door centroid markings at the top and bottom of each door to serve as highly relevant spatial anchors for subsequent segmentation.

3.3 Preprocessing: Corridor isolation

In indoor PCD processing, corridors pose a unique challenge due to their geometric nature of being elongated and having multiple connections to numerous individual indoor spaces. Accordingly, the proposed framework implements a corridor-specific segmentation algorithm that identifies and processes corridors for easier segmentation among indoor spaces. The corridor detection algorithm utilizes the slices created from the prior door seed detection step. First, the wall slices are used to extract wall boundaries associated with corridor by filtering vertical planes using Principal Component Analysis (PCA) (Eq. (3).), where n_i is the plane normal and c_i is the centroid.

$$n_i \cdot (p - c_i) = 0 \quad (3)$$

Second, the algorithm computes the corridor axis by fitting a line through door centroids $\{d_i\}$, again using PCA, keeping only the first principle component (Eq. (4).), where PCA_1 returns the top eigenvector (direction) of the given set of points.

$$axis = PCA_1(\{d_i\}) \quad (4)$$

Third, the lateral boundaries are defined using the fitted wall planes to constrain the corridor region. Last, a region

growing is implemented from the initial corridor core (e.g., midpoints along *axis*), while preserving the additional points comply the three conditions: 1) lateral contamination within the wall boundaries defined by the planes $\{n_i, c_i\}$, and 2) planarity constraint floors/ceilings (Eq. (5).), where $n_z(p)$ is the z-component of the estimated normal at point p :

$$|n_z(p)| > \cos(30^\circ) \quad (5)$$

And 3) connectivity to the corridor region (e.g., 4 or 8 connected in the 2D grid projection). The isolated corridor segments are temporarily removed to prevent interference with room segmentation and then reintegrated in the final labeling stage.

3.4 Preprocessing: Structural filtering

The structural filtering algorithm divides the point cloud into overlapping tiles of size $T \times T$ (where $T=1.0m$) with overlap $\tau=0.1m$ to ensure continuity across tile boundaries. For each tile T_{ij} , the algorithm performs multi-stage analysis to classify and filter structural components through a series of geometric computations: 1) For each point p_i , let N_i denote its k-nearest-neighbor set and compute the covariance matrix of N_i , then take the eigenvector corresponding to the smallest eigenvalue, which yields the surface normal n_i (Eq. (6).).

$$n_i = \text{eigenvector}(\lambda_{min}, COV(N_i)) \quad (6)$$

2) Compute the magnitude of the z-component of each normal by setting $\theta_h = 12^\circ$ to be the horizontal angle threshold, which means any point whose normal satisfies $|n_z \geq \cos(\theta_h)|$ is either floor or ceiling. 3) Extract vertical planes by adaptively implementing RANSAC for indoor environments (min. inliers: 100 points, dist. threshold: 0.1m, max. iterations: 1,000). 4) Remove tiny clusters (furniture, artifacts, etc.) that could interfere with boundary detection.

3.5 Preprocessing: Verticality and analysis/merging

The final preprocessing step separates walls from horizontal surfaces based on verticality analysis, while incorporating door seed information to ensure complete boundary representation. The structurally filtered point cloud from Section 3.4 is utilized to produce the final wall mask for subsequent segmentation. First, verticality v is computed for each surface point by taking the absolute value of the z-component of its normal n by setting $e_z = (0,0,1)^T$ (Eq. (7).).

$$v = |n_z| = |n \cdot e_z| \quad (7)$$

Points are classified as follows: 1) if $v < 0.2$, wall points and if $v \geq 0.2$, floor/ceiling points. These thresholds account for slight wall inclinations and surface irregularities. As the final processing step, classified wall points are merged with door seeds from Section 3.2.

3.6 Indoor space segmentation: Enhanced wall mask generation

Following preprocessing, the first segmentation step creates a refined 2D occupancy grid representing vertical structures by integrating both 2D density distributions and 3D geometric constraints. This approach addresses limitations of pure height-based filtering, especially in scenarios with high doorways or partial walls, which are common in forensic-engineering contexts, where the grid resolution g is set to be 0.05m and 2D occupancy grid G_{ij} is defined as Eq. (8.).

$$G_{ij} = \{p \in P : |p_x/g| = i, |p_y/g| = j\} \quad (8)$$

For each occupied cell (i, j) , multi-criteria validation is performed to examine if a cell contains a wall point: 1) any point with elevation $z < 1.0$ m and total vertical span $\Delta z \geq 0.8$ m for standard wall detection, and 2) any point with $z \geq 1.0$ m and height span $\Delta z \geq 0.5$ m for high-doorway detection, and 3) sufficient point density check to distinguish between real walls from sparse artifacts. An adaptive KD-tree query is performed with search radius $r = g * 2.0$ to support the above three validations. In other words, a binary indicator is introduced (Eq. (9)).

$$V_{ij} = \begin{cases} 1, & \text{if at least one of (1) - (3) holds in cell } (i, j) \\ 0, & \text{otherwise} \end{cases} \quad (9)$$

After obtaining V , 2D density filtering is applied to remove detections arising from noise or non-wall structures by enforcing: 1) minimum component area $A_{min} = \ell_{min} * w_{min}$, where $\ell_{min} = 0.25$ m and $w_{min} = 0.08$ m, and minimum point density of 2 points per cell. The final wall mask undergoes morphological refinement to ensure spatial coherence (Eq. (10).), where ψ represents the closing operation with disk (4) structural element and ϕ represents the opening operation with disk (1) structural element.

$$W_{final} = \phi(\psi(W_{filtered})) \quad (10)$$

3.7 Indoor space segmentation: Adaptive anchor seed extraction

The second segmentation step identifies optimal anchor seeds for watershed segmentation by analyzing free-space distribution while respecting building boundary constraints and door locations. First, establish the building envelope B through multi-modal analysis: 1) form an occupancy grid from floor points to identify the indoor extent for floor density mapping, 2) apply the 25th-percentile threshold to discard cells with insufficient density for statistical filtering, 3) close gaps and fill interior holes to produce a continuous boundary for morphological operations, and 4) combine floor-derived boundary with wall-derived boundary to get a robust mask B . The constrained free space F is defined by Eq. (11.), where W is the binary wall mask from Eq. (10).

$$F = \neg W \wedge B \quad (11)$$

The Euclidean distance transform is subsequently calculated on the constrained free space to quantify the

distance from each free space pixel to the nearest wall or boundary (Eq. (12).), where the computed distances are scaled by the grid resolution to maintain metric consistency.

$$D(i, j) = \min_{(i', j')} ||(i, j) - (i', j')|| \times g \quad (12)$$

Local maxima in the distance transform serve as initial anchor candidates for room centers, identified through neighborhood comparison (Eq. (13).), where $d_{thresh.} = (0.5, 0.3 \times \max(D))$ provides an adaptive threshold based on the maximum distance value, and N_{ij} represents the 8-connected neighborhood of pixel (i, j) .

$$C = (i, j) : D(i, j) > D(N_{ij}), D(i, j) \geq d_{thresh} \quad (13)$$

The adaptive filtering process subsequently refines the candidate set by ensuring minimum separation of 0.4m between anchors to prevent over-segmentation, prioritizing door seed injection with artificially elevated distance values to ensure room boundaries align with detected doors, and guaranteeing coverage of all significant regions through iterative erosion-based analysis that identifies isolated spaces requiring additional anchors.

3.8 Indoor space segmentation: Hierarchical watershed with spillage prevention

The third and final segmentation method implements an enhanced watershed algorithm incorporating multiple spillage prevention mechanisms to achieve accurate room segmentation even in architecturally complex layouts. This module specifically addresses the over-segmentation issues prevalent in traditional watershed methods through hierarchical contour analysis and multi-scale morphological processing.

The hierarchical contour analysis begins by extracting wall contours from the binary wall mask and constructing a hierarchy tree to understand nested spatial relationships. This process involves four sequential steps: 1) extracting contours from the wall mask using connected component analysis, 2) building parent-child relationships from the extracted hierarchy to identify nested structures, 3) classifying regions as either outer boundaries or nested spaces based on their nesting level within the hierarchy, and 4) identifying special configurations such as ring corridors and complex nested structures that require specialized handling.

Multi-scale morphological separation addresses the challenge of varying opening sizes through the application of multiple erosion scales. The algorithm employs four distinct scales: narrow doors utilize $r_1 = 0.09$ m (representing 60% of standard door width), standard door employ $r_2 = 0.15$ m, wide openings use $r_3 = 0.225$ m, and large space apply $r_4 = 0.30$ m. This multi-scale approach ensures proper spatial separation regardless of the specific opening dimensions present in the structure. The enhanced watershed implementation incorporates several algorithmic innovations to improve segmentation accuracy. Conservative marker placement is implemented through a tri-state labeling scheme (Eq. (14)).

$$M_{ij} \begin{cases} -1, & \text{if } w_{ij} = 1 \text{ (wall cell),} \\ \ell, & \text{if } (i,j) \in A_\ell \pm \text{ (dilated neigh. of anchor } \ell\text{),} \\ 0, & \text{otherwise} \end{cases} \quad (14)$$

where A_ℓ represents the dilated neighborhood of anchor ℓ to ensure robust marker placement. Enhanced barrier strength for the watershed algorithm is computed by combining distance transform values with exponential wall proximity weighting (Eq. (15).), where d_{wall} represents the distance from the nearest wall, $\alpha = 0.4$ controls the barrier strength contribution, and $\sigma = 2.5$ determines the spatial extent of wall influence.

$$I_{watershed} = \max(D) - D + \alpha \exp(-d_{wall}/\sigma) \quad (15)$$

Spillage detection and correction mechanisms continuously monitor room areas during the segmentation process, automatically flagging rooms that exceed 80m² for potential subdivision, applying intelligent subdivision based on secondary peaks in the distance transform, and implementing distance-based trimming for regions that extend beyond reasonable boundaries. Additionally, aggressive unlabeled pixel assignment ensures comprehensive spatial coverage by assigning pixels within 5 cells of existing room boundaries, creating new room segments for unlabeled regions exceeding 4 m² in area, and applying nearest-neighbor assignment for any remaining unlabeled pixels.

3.9 Post-segmentation

The final stage of the framework applies several refinement procedures designed to improve segmentation quality and ensure the practical usability of results for forensic engineering applications.

Small fragmented rooms resulting from potential over-segmentation are systematically merged based on three complementary criteria. The size threshold identifies rooms with area less than 6 m² as candidates for merging, recognizing that such small spaces are unlikely to represent actual rooms in typical architectural configurations. Adjacency analysis examines the spatial relationships between merge candidates and their neighboring rooms, selecting the largest adjacent room as the merge target to maintain spatial coherence. Shape regularity assessment ensures that the resulting merged rooms form geometrically reasonable spaces, preventing the creation of highly irregular or non-convex configurations that would be architecturally implausible.

The 6m² size threshold derives from architectural standards and empirical analysis. Building codes typically specify minimum room sizes of 7 m² for habitable spaces, with service rooms ranging from 2-5 m². The 6m² threshold thus captures the boundary between legitimate small rooms and segmentation artifacts. Empirical validation on the S3DIS dataset confirmed that regions below this threshold predominantly represented over-segmentation artifacts rather than actual rooms, with 89% of sub-6 m² regions resulting from watershed spillage at doorways or partial wall segments. This threshold ensures consolidation of fragmented segments while preserving legitimate small

spaces such as storage rooms and bathrooms.

The 2D segmentation results obtained from the previous stages are mapped back to the original 3D floor points to produce the final room-level point cloud segmentation (Eq. (16).).

$$L_i = G\left\{\left[\left[\frac{p_{(ix)}}{g}\right], \left[\frac{p_{(iy)}}{g}\right]\right]\right\} \quad (16)$$

Final 3D cleanup operations remove tiny room artifacts containing less than 0.1% of the total point count and systematically renumber rooms consecutively for clarity and ease of interpretation. These cleanup operations ensure that the output segmentation is suitable for downstream applications including BIM generation and forensic damage assessment.

4. Validations and results

This chapter evaluates the proposed framework using room-level Intersection over Union (IoU), F1-score, and precision metrics. The IoU measures spatial overlap between predicted and ground truth rooms, calculated as the intersection divided by the union of point sets. The F1-score provides balanced assessment through the harmonic mean of precision and recall. Precision represents the fraction of predicted room points that correctly match ground truth assignments. These metrics evaluate room-level correspondence rather than point-wise accuracy, aligning with the framework's objective of identifying spatially coherent rooms for forensic assessment. The proposed door-guided indoor space segmentation framework was validated using Area 6 of the S3DIS dataset, which contains large-scale indoor point clouds with semantic annotations. The test dataset comprised a consolidated point cloud representing 27 individual rooms from a multi-story building, containing 1,168,342 points in total. This dataset was selected due to its architectural complexity, including narrow corridors, varying room sizes, and diverse structural configurations that challenge traditional segmentation approaches.

The preprocessing pipeline successfully processed the raw point cloud through four sequential modules, establishing critical spatial boundaries for subsequent segmentation. The door detection module accurately identified all door point seed pairs and their corresponding wall slices within the building structure. A total of 60 door seed points were detected, representing 30 door openings distributed throughout the building. Each door opening was characterized by paired top and bottom centroid markings, providing robust spatial anchors for the subsequent segmentation phases. The geometric validation criteria successfully filtered candidate gaps, ensuring that only legitimate door openings with heights between 1.6 m and 2.5 m and widths between 0.7 m and 1.2 m were retained (Fig. 2.).

The corridor isolation module effectively identified and segmented the building's corridor system, achieving strong performance metrics as shown in Fig. 3.

The algorithm successfully detected the primary corridor axis and established lateral boundaries through planar fitting of associated wall segments. The isolated corridor regions demonstrated precision of 0.990, recall of

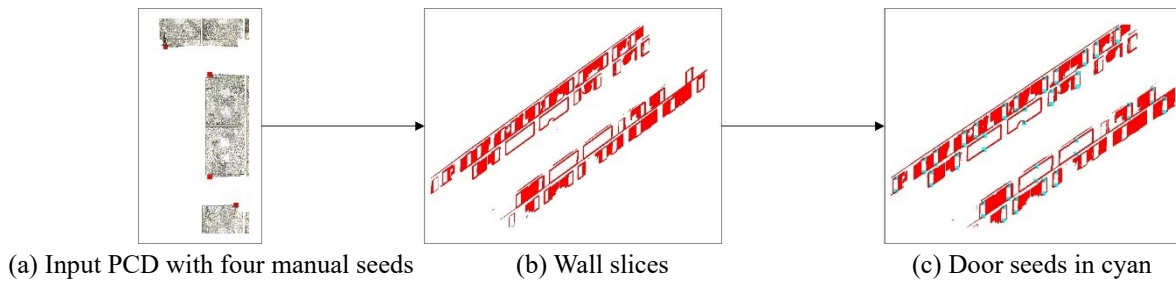


Fig. 2 Door seed detection

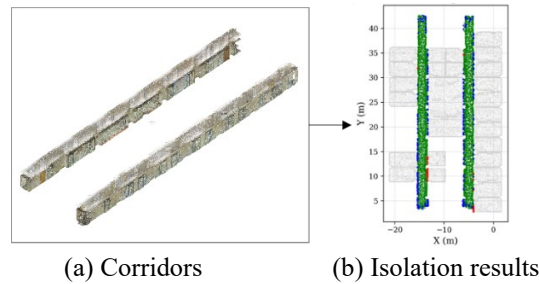


Fig. 3 Corridor isolation/segmentation

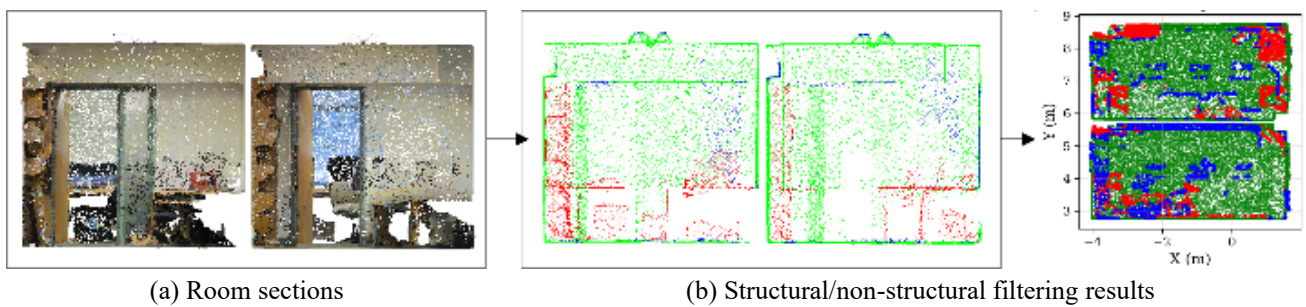


Fig. 4 Structural filtering

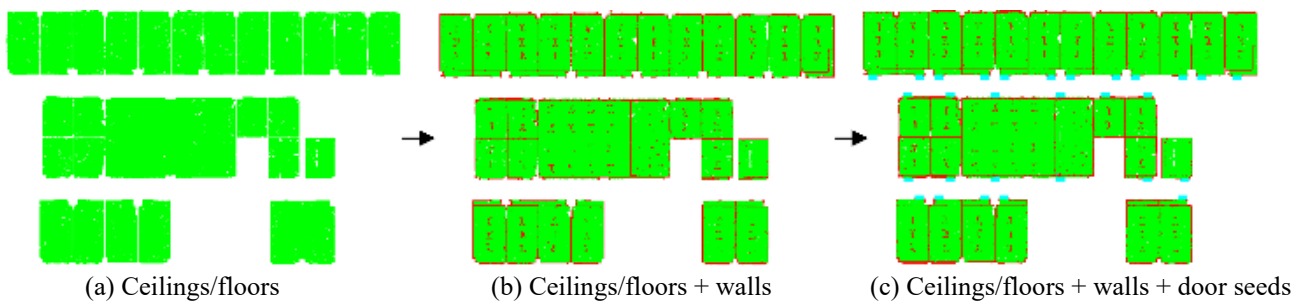


Fig. 5 Verticality analysis and merging

0.947, and an F1-score of 0.968, indicating robust identification of elongated circulation spaces. The temporarily removed corridor segments comprised approximately 15% of the total floor area, substantially simplifying the subsequent room segmentation task.

The structural filtering module distinguished load-bearing elements from non-structural components, achieving the performance metrics illustrated in Fig. 4. The tile-based approach processed 1,049,750 total points, correctly classifying 75,627 as structural elements with precision of 0.902 and recall of 0.933. While the achieved accuracy of 0.865 fell short of perfect classification, this

performance level satisfied the module's primary objective of reducing clutter interference in subsequent segmentation stages. The filtering process successfully removed furniture artifacts and other non-structural elements that would otherwise complicate boundary detection, with the understanding that absolute accuracy was not the goal but rather the creation of cleaner input data for room segmentation.

The verticality analysis module computed surface normals for all structural points and classified them based on the absolute value of their z-component. Points exhibiting verticality values below 0.2 were classified as

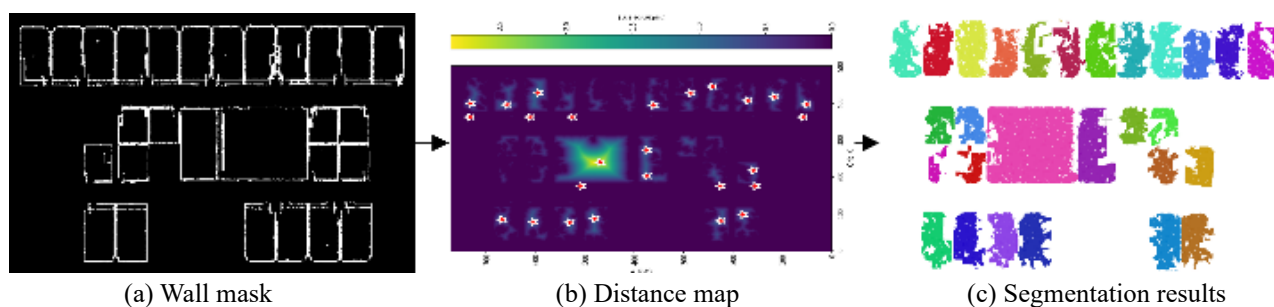


Fig. 6 Indoor Space Segmentation

Table 1 Room-by-room performance metrics

	IoU	F-1 Score	Area m^2
Room 1	0.952	0.962	41.0
Room 2	0.888	0.975	6.4
Room 3	0.978	0.941	8.7
Room 4	0.971	0.989	8.3
Room 5	0.968	0.985	6.4
Room 6	0.974	0.984	8.9
Room 7	0.945	0.987	7.2
Room 8	0.983	0.972	7.9
Room 9	0.969	0.991	6.8
Room 10	0.938	0.984	7.5
Room 11	0.966	0.983	8.1
Room 12	0.973	0.986	6.9
Room 13	0.982	0.991	9.8
Room 14	0.967	0.983	7.3
Room 15	0.985	0.992	8.6

walls, while those exceeding this threshold were designated as horizontal surfaces. The analysis successfully separated 558,947 wall points from 237,659 floor points, achieving clear delineation between vertical and horizontal structures. The classified wall points were subsequently merged with the 60 door seed points through grid projection and morphological operations, producing a comprehensive wall mask that preserved door gaps while ensuring structural connectivity (Fig. 5.).

This merged point cloud, containing both wall boundaries and door markers, served as the primary input for the final segmentation phase. The indoor space segmentation phase processed the preprocessed data through three integrated steps to achieve room-level partitioning. The first step established a 2D occupancy grid with dimensions of 503×772 cells at 0.05m resolution. The enhanced height filtering successfully identified 28,638 wall cells, representing 16.8% of the total grid area. The module's multi-criteria validation detected 696,593 vertical structure points from the input data. Component-based filtering removed 11 spurious detections based on density and area constraints, retaining 17 valid wall components. The improved height filtering specifically addressed high doorway scenarios, ensuring continuous wall detection even for openings extending above the 1.0 m threshold.

The second module computed the building boundary through multi-modal analysis, establishing a boundary coverage of 160,788 cells. The distance transform analysis revealed a maximum distance of 2.87 m from walls, with adaptive thresholds set at 0.57m for anchor filtering. Initial local maxima detection identified 100 candidates, which were refined to 35 anchor seeds through separation filtering. Seven door seeds were injected as high-priority anchors, bringing the total to 42 anchor seeds. The comprehensive region coverage analysis identified 69 regions at the finest erosion scale, progressively reducing to 21 regions at the coarsest scale, ensuring adequate coverage of all significant spaces.

The third module processed 35 detected contours, classifying them into 4 outer regions and 31 nested regions within the hierarchical structure. Multi-scale morphological separation tested four erosion radii, ultimately selecting the wide_openings configuration with 29 regions for optimal separation. The enhanced watershed implementation created 28 standard markers with strengthened barriers to prevent spillage. Post-watershed analysis identified one large room (Room 1) spanning 41 m^2 , which was retained without subdivision based on architectural coherence. The final segmentation produced 27 distinct rooms with size averaging 7.5 m^2 excluding the large central space (Fig. 6).

The segmentation results were evaluated against 27 ground truth rooms through floor-to-floor comparison, as presented in Table 1. for first fifteen results. The framework achieved an average Intersection over Union (IoU) of 0.965, with F1-scores averaging 0.980. Individual room performance demonstrated consistently high accuracy, with Room 2 achieving the minimum IoU of 0.888 (matched with ground truth Room 26), while most rooms exceeded 0.95 IoU. Average precision reached 98.0%.

5. Conclusions

This study proposed a novel door-guided indoor space segmentation framework for large-scale point clouds that addresses the limitations of existing methods through a purely geometric approach. The framework eliminates dependence on learned features while maintaining high segmentation accuracy, making it particularly suitable for forensic engineering applications where training data is scarce and computational resources are limited. The following sections discuss the key findings, limitations, and future research directions.

5.1 Key research findings

The primary innovation of this research lies in the development of a preprocessing-first approach that establishes robust spatial boundaries before applying volumetric partitioning. Unlike existing methods that rely on pre-trained neural networks or suffer from parameter sensitivity, the proposed framework implements purely geometric door gap detection through cross-sectional analysis and density-based filtering. The door detection module successfully identified all 60 door seed points representing 30 door openings, providing reliable spatial anchors without requiring any training data.

The four-module preprocessing pipeline demonstrated exceptional effectiveness in preparing point clouds for segmentation. The corridor isolation module achieved precision of 0.990, recall of 0.947, and F1-score of 0.968, successfully removing approximately 15% of the total floor area that would otherwise complicate room segmentation. The structural filtering module processed 1,049,750 points with precision of 0.902 and recall of 0.933, effectively removing non-structural elements that interfere with boundary detection. The verticality analysis successfully separated 558,947 wall points from 237,659 floor points, producing a comprehensive wall mask that preserved door gaps while ensuring structural connectivity.

The indoor space segmentation phase achieved remarkable performance on the S3DIS Area 6 dataset. The framework successfully segmented 27 rooms from a consolidated point cloud of 1,168,342 points, achieving an average IoU of 0.965 and F1-score of 0.980 across all detected rooms. This performance substantially exceeds typical geometry-based methods while avoiding the computational overhead and data dependencies of learning-based approaches.

5.2 Limitations and future research directions

While the proposed framework demonstrates strong performance, several limitations warrant acknowledgment and future investigation. The reliance on manually marked door seed points, though eliminating training data dependencies, requires initial human input. However, this input is minimal (only 4 clicks total for an entire building), and could be further automated through geometric heuristics or lightweight detection algorithms. The current implementation assumes door openings conform to standard dimensions (1.6-2.5m height, 0.7-1.2m width), potentially missing non-standard openings in unconventional architectural designs.

The framework was validated solely on Area 6 of the S3DIS dataset, representing 27 rooms in a single building. Further validation across diverse architectural styles, building types, and cultural contexts is necessary to establish generalizability. Forensic engineering applications often involve damaged or partially collapsed structures where door openings may be obstructed or deformed, presenting challenges not addressed in the current validation.

Future research should explore several promising directions. Integration of the framework with automated door detection using geometric features rather than learned models could eliminate manual input while maintaining the purely geometric approach. Extension to multi-story buildings with stairwells and elevators requires adaptation of the corridor isolation module to handle vertical circulation spaces. Investigation of adaptive parameter selection based on building typology could further improve robustness across diverse architectural configurations.

The framework's application to forensic damage assessment scenarios requires specific enhancements. Development of modules to handle partial structural collapse, debris fields, and deformed openings would extend applicability to post-disaster scenarios. Integration with temporal point cloud data could enable change detection and progressive damage assessment. Coupling with structural analysis tools could provide comprehensive forensic investigation capabilities, from spatial segmentation to damage quantification.

5.3 Conclusion

This research successfully developed and validated a door-guided indoor space segmentation framework that advances the state-of-the-art in purely geometric approaches. By introducing explicit door gap detection, tile-based structural filtering, corridor-specific segmentation, and hierarchical watershed partitioning with spillage prevention, the framework addresses critical limitations identified in existing methods. The achieved average IoU of 0.965 and F1-score of 0.980 demonstrate that geometry-based methods can match or exceed the performance of learning-based approaches when properly designed with architectural constraints in mind.

The framework's significance extends beyond technical metrics to practical applicability in forensic engineering

contexts. The elimination of training data requirements, computational efficiency enabling standard hardware deployment, and modular design supporting parameter adaptation make it particularly suitable for field conditions where resources are constrained and architectural configurations vary. The preprocessing-first philosophy ensures robust spatial boundaries are established before segmentation, reducing sensitivity to parameter selection and improving consistency across diverse scenarios.

In practice, the framework enables straightforward deployment for forensic engineering applications. Field engineers capture point clouds using mobile LiDAR or photogrammetry with standard RGB attributes, requiring only minimal door location marking through an efficient geometric prediction system. By clicking once at each end of the four main building axes (4 clicks total), the framework automatically identifies door positions for all rooms aligned along these corridors, eliminating the need for individual door marking. The framework executes on standard field laptops without GPU requirements, processing typical 50-room buildings (~5 million points) in under 2 minutes. This enables immediate quality verification and re-scanning if needed.

Output room segments export directly to IFC format, enabling seamless integration with BIM authoring tools (Revit, ArchiCAD) and facility management systems. Each room receives a unique identifier for linking to inspection databases. The room-level segmentation supports: a) automated floor plan generation for emergency response, b) damage extent quantification by affected room area, c) temporal change detection through periodic re-scanning, and d) spatially-indexed inspection reports where defects link to specific rooms. Current limitations include the requirement for manual door marking, though ongoing work explores automatic door detection through geometric heuristics. Complex atriums exceeding 200m² may require manual subdivision, which future interactive refinement tools will address.

This work contributes to the broader objective of enabling Forensic Information Modeling (FIM) through accurate and efficient point cloud processing. By facilitating rapid room-level segmentation of as-damaged structures, the framework enhances forensic engineers' capability to assess structural integrity, document damage patterns, and communicate findings to diverse stakeholders. The integration potential with BIM workflows and damage assessment tools positions this framework as a critical component in the evolving landscape of digital forensic engineering, supporting more efficient investigations, accurate documentation, and informed decision-making in post-disaster scenarios.

Acknowledgements

This work was supported by the National Research Foundation of Korea (NRF) grant funded by the Korea government (MSIT) (No. RS-2021-NR060085).

References

- Bae, S.J. and J.Y. Kim (2023), "Indoor clutter object removal method for an as-built building information model using a two-dimensional projection approach", *Appl. Sci.*, **13**(17), 9636. <https://doi.org/10.3390/app13179636>.
- Brando, F., Iannitelli, A., Cao, L., Malsch, E.A., Panariello, G., Abruzzo, J. and Pinto, M.J. (2013), "Forensic Information Modeling for infrastructure assessment", *J. Perform. Construct. Facilities*, **27**(3), 294-307.
- Chen, J., Liu, C., Wu, J. and Furukawa, Y. (2019), "Floor-sp: Inverse cad for floorplans by sequential room-wise shortest path", *Proceedings of the IEEE/CVF International Conference on Computer Vision*, 2661-2670.
- Coughlan, J. and Yuille, A.L. (1999), "Manhattan World: Compass direction from a single image by Bayesian inference", *Proceedings International Conference on Computer Vision ICCV'99*, 941-947.
- Dasgupta, S., Fang, K., Chen, K. and Savarese, S. (2016), "Delay: Robust spatial layout estimation for cluttered indoor scenes", *Proceedings of the IEEE Conference on Computer Vision and Pattern Recognition*, 616-624.
- Fabbri, R., Costa, L.D.F., Torelli, J.C. and Bruno, O.M. (2008), "2D euclidean distance transform algorithms: A comparative survey", *ACM Computing Surveys* **40**(1), 1-44. <https://doi.org/10.1145/1322432.1322434>.
- Fang, H., Lafarge, F., Pan, C. and Huang, H. (2021), "Floorplan generation from 3D point clouds: A space partitioning approach", *ISPRS J. Photogrammetry Remote Sensing*, **175**, 44-55. <https://doi.org/10.1016/j.isprsjprs.2021.02.012>.
- Gong, X.-Y., Su, H., Xu, D., Zhang, Z.-T., Shen, F. and Yang, H.-B. (2018), "An overview of contour detection approaches", *Int. J. Automation Comput.*, **15**, 656-672. <https://doi.org/10.1007/s11633-018-1117-z>.
- He, K., Gkioxari, G., Dollár, P. and Girshick, R. (2017), "Mask r-cnn", *Proceedings of the IEEE International Conference on Computer Vision*, 2961-2969.
- Hu, D., Gan, V.J.L. and Zhai, R. (2024), "Automated BIM-to-scan point cloud semantic segmentation using a domain adaptation network with hybrid attention and whitening (DawNet)", *Automation Construct.*, **164**, 105473. <https://doi.org/10.1016/j.autcon.2024.105473>.
- Hübner, P., Weinmann, M., Wursthorn, S. and Hinz, S. (2021), "Automatic voxel-based 3D indoor reconstruction and room partitioning from triangle meshes", *ISPRS J. Photogrammetry Remote Sensing*, **181**, 254-278. <https://doi.org/10.1016/j.isprsjprs.2021.07.002>.
- Jung, J., Stachniss, C. and Kim, C. (2017), "Automatic room segmentation of 3D laser data using morphological processing", *ISPRS Int. J. Geo-Inform.*, **6**(7), 206. <https://doi.org/10.3390/ijgi6070206>.
- Kim, M., Lee, D., Kim, T., Oh, S. and Cho, H. (2023), "Automated extraction of geometric primitives with solid lines from unstructured point clouds for creating digital buildings models", *Automation Construct.*, **145**, 104642. <https://doi.org/10.1016/j.autcon.2022.104642>.
- Lee, C.Y., Badrinarayanan, V., Malisiewicz, T. and Rabinovich, A. (2017), "Roomnet: End-to-end room layout estimation", *Proceedings of the IEEE International Conference on Computer Vision*, 4865-4874.
- Li, L., Chen, J., Su, X., H. Han, and C. Fan. 2024. "Deep learning network for indoor point cloud semantic segmentation with transferability." *Automation in Construction* 168: 105806. <https://doi.org/10.1016/j.autcon.2024.105806>.
- Li, L., F. Su, F. Yang, H. Zhu, D., Li, X., Zuo, F., Li, and Ying, S. (2018), "Reconstruction of three-dimensional (3D) indoor interiors with multiple stories via comprehensive segmentation",

- Remote Sensing*, **10**(8), 1281. <https://doi.org/10.3390/rs10081281>.
- Liu, C., Wu, J. and Furukawa, Y. (2018), "FloorNet: A unified framework for floorplan reconstruction from 3D scans", *In Computer Vision – ECCV 2018*, 203-219. https://doi.org/10.1007/978-3-030-01231-1_13.
- Liu, C., Wu, J., Kohli, P. and Furukawa, Y. (2017), "Raster-to-vector: Revisiting floorplan transformation", *Proceedings of the IEEE International Conference on Computer Vision*, 2195-2203.
- Ma, J., W., Czerniawski, T. and Leite, F. (2020), "Semantic segmentation of point clouds of building interiors with deep learning: Augmenting training datasets with synthetic BIM-based point clouds", *Automation Construct.*, **113**, 103144. <https://doi.org/10.1016/j.autcon.2020.103144>.
- Mahmoud, M., Zhao, Z., Chen, W., Adham, M. and Li, Y. (2025), "Automated scan-to-BIM: A deep learning-based framework for indoor environments with complex furniture elements", *J. Build. Eng.*, **106**, 112596. <https://doi.org/10.1016/j.job.2025.112596>.
- Nikoohemat, S., Diakité, A.A., Zlatanova, S. and Vosselman, G. (2020), "Indoor 3D reconstruction from point clouds for optimal routing in complex buildings to support disaster management", *Automation Construct.*, **113**, 103109. <https://doi.org/10.1016/j.autcon.2020.103109>.
- Ochmann, S., Vock, R. and Klein, R. (2019), "Automatic reconstruction of fully volumetric 3D building models from oriented point clouds", *ISPRS J. Photogrammetry Remote Sensing*, **151**, 251-262. <https://doi.org/10.1016/j.isprsjprs.2019.03.017>.
- Ochmann, S., Vock, R., Wessel, R. and Klein, R. (2016), "Automatic reconstruction of parametric building models from indoor point clouds", *Comput. Graphics*, **54**, 94-103. <https://doi.org/10.1016/j.cag.2015.07.008>.
- Park, J., Kim, J., Lee, D., Jeong, K., Lee, J., Kim, H. and Hong, T. (2022), "Deep learning-based automation of scan-to-BIM with modeling objects from occluded point clouds", *J. Manage. Eng.*, **38**(4), 04022025. [https://doi.org/10.1061/\(ASCE\)ME.1943-5479.0001055](https://doi.org/10.1061/(ASCE)ME.1943-5479.0001055).
- Patil, J. and Kalantari, M. (2025), "Automatic scan-to-BIM—The impact of semantic segmentation accuracy", *Buildings*, **15**(7), 1126. <https://doi.org/10.3390/buildings15071126>.
- Perez-Perez, Y., Golparvar-Fard, M. and El-Rayes K. (2021), "Scan2BIM-NET: Deep learning method for segmentation of point clouds for scan-to-BIM", *J. Construct. Eng. Manage.*, **147**(9), 04021107. [https://doi.org/10.1061/\(ASCE\)CO.1943-7862.0002132](https://doi.org/10.1061/(ASCE)CO.1943-7862.0002132).
- Poux, F., Mattes, C., Selman, Z. and Kobbelt, L. (2022), "Automatic region-growing system for the segmentation of large point clouds", *Automation Construct.*, **138**, 104250. <https://doi.org/10.1016/j.autcon.2022.104250>.
- Ronneberger, O., Fischer, P. and Brox, T. (2015), "U-net: Convolutional networks for biomedical image segmentation", *In Medical Image Computing and Computer-Assisted Intervention—MICCAI 2015*, 234-241. Springer.
- Sahin, C. (2015), "Planar segmentation of indoor terrestrial laser scanning point clouds via distance function from a point to a plane", *Optics Lasers Eng.*, **64**, 23-31. <https://doi.org/10.1016/j.optlaseng.2014.07.007>.
- Singh, V.P. and Frevert, D.K. (2003), "Watershed modeling", *World Water Environmental Resources Congress*, **2003**, 1-37.
- Song, S.H., Ahn, H., Lee, C., Kim, H., Yun, T.S., Zi, G. and Cho, H. (2024), "Guided segmentation of large-scale indoor spaces using door point clusters", *Steel Compos. Struct.*, **53**(6), 677. <https://doi.org/10.12989/scs.2024.53.6.677>.
- Tang, S., Huang, J., Cai, B., Du, H., Zhou, B., Zhao, Z., Li, Y., Wang, W. and Guo, R. (2024), "Back to geometry: Efficient indoor space segmentation from point clouds by 2D–3D geometry constrains", *Int. J. Appl. Earth Observation*, **135**, 104265. <https://doi.org/10.1016/j.jag.2024.104265>.
- Tang, S., Li, X., Zheng, X., Wu, B., Wang, W. and Zhang, Y. (2022), "BIM generation from 3D point clouds by combining 3D deep learning and improved morphological approach", *Automation Construct.*, **141**, 104422. <https://doi.org/10.1016/j.autcon.2022.104422>.
- Thomson, C. and Boehm, J. (2015), "Automatic geometry generation from point clouds for BIM", *Remote Sensing*, **7**(9), 11753-11775. <https://doi.org/10.3390/rs70911753>.
- Tran, H. and Khoshelham, K. (2020), "Procedural reconstruction of 3D indoor models from lidar data using reversible jump Markov chain Monte Carlo", *Remote Sensing*, **12**(5), 838. <https://doi.org/10.3390/rs12050838>.
- Wang, C., Cho, Y.K. and Kim, C. (2015), "Automatic BIM component extraction from point clouds of existing buildings for sustainability applications", *Automation Construct.*, **56**, 1-13. <https://doi.org/10.1016/j.autcon.2015.04.001>.
- Wang, Q. and Kim, M.K. (2019), "Applications of 3D point cloud data in the construction industry: A fifteen-year review from 2004 to 2018", *Adv. Eng. Inform.*, **39**, 306-319. <https://doi.org/10.1016/j.aei.2019.02.007>.
- Yang, J., Kang, Z., Zeng, L., Hope Akwensi, P. and Sester, M. (2021), "Semantics-guided reconstruction of indoor navigation elements from 3D colorized points", *ISPRS J. Photogrammetry Remote Sensing*, **173**, 238-261. <https://doi.org/10.1016/j.isprsjprs.2021.01.013>.